Article

An efficient gene targeting system using Δ*ku80* and functional analysis of Cyp51A in *Trichophyton rubrum*

Masaki Ishii[*,a], Tsuyoshi Yamada[b,c], and Shinya Ohata[*,a]

[a]Research Institute of Pharmaceutical Sciences, Faculty of Pharmacy, Musashino University, Tokyo 202-8585, Japan

[b]Teikyo University Institute of Medical Mycology, Teikyo University, Hachioji, Tokyo 192-0395, Japan

[c]Asia International Institute of Infectious Disease Control, Teikyo University, Tokyo, Japan

[*] Correspondence e-mail: m_ishii@musashino-u.ac.jp, shiohata@musashino-u.ac.jp

ORCID

Masaki Ishii, 0000-0003-0687-3147; Tsuyoshi Yamada, 0000-0002-1394-5455; Shinya Ohata, 0000-0003-4333-4433

Abstract: (248 words)

Trichophyton rubrum is one of the most frequently isolated fungi in patients with dermatophytosis. Despite its clinical significance, the molecular mechanisms of drug resistance and pathogenicity of *T. rubrum* remain to be elucidated because of the lack of genetic tools, such as efficient gene targeting systems. In this study, we generated a *T. rubrum* strain that lacks the nonhomologous end-joining-related gene *ku80* (Δ*ku80*) and then developed a highly efficient genetic recombination system with gene targeting efficiency that was 46 times higher than that using the wild-type strain. Cyp51A and Cyp51B are 14-α-lanosterol demethylase isozymes in *T. rubrum* that promote ergosterol biosynthesis and are the targets of azole antifungal drugs. The expression of *cyp51A* mRNA was induced by the addition of the azole antifungal drug efinaconazole, whereas no such induction was detected for *cyp51B*, suggesting that Cyp51A functions as an azole-responsive Cyp51 isozyme. To explore the contribution of Cyp51A to susceptibility to azole drugs, the neomycin phosphotransferase (*nptII*) gene cassette was inserted into the *cyp51A* 3′-UTR region of Δ*ku80* to destabilize the mRNA of *cyp51A*. In this mutant, although the expression level of *cyp51A* mRNA was comparable to that of the parent strain, the induction of *cyp51A* mRNA expression by efinaconazole was diminished. The minimum inhibitory concentration for several azole drugs of this strain was reduced, suggesting that dermatophyte Cyp51A contributes to the tolerance for azole drugs. These findings suggest that an efficient gene targeting system using Δ*ku80* in *T. rubrum* is applicable for analyzing genes encoding drug targets.

Keywords

Dermatophyte, *Trichophyton rubrum*, Ku80, Cyp51A

Statements and Declarations

Authors have no competing interests.

Key Points (3 key points have less than 86 characters)

1. A novel gene targeting system using Δ*ku80* strain was established in *T. rubrum*
2. Cyp51A in *T. rubrum* responds to the azole antifungal drug efinaconazole
3. Cyp51A contributes to azole drug tolerance in *T. rubrum*

INTRODUCTION

Dermatophytosis is a superficial fungal infection with symptoms such as itching, redness, and nail abnormalities. Tinea pedis (athlete's foot), a type of dermatophytosis, affects approximately 10% of the world's population (1). *Trichophyton rubrum*, the most common dermatophyte (2), is a clinically important organism that reduces the quality of life and has a unique life cycle as an anthropophilic dermatophyte that specifically inhabits human surface tissues. A limited class of antifungals, such as azole antifungals, are used in dermatophytosis treatment. Although drug resistance issues in *T. rubrum* have resulted in a need to elucidate the detailed molecular mechanisms of its drug resistance and identify and analyze drug targets (3, 4), these issues have not been completely clarified because of the underdevelopment of genetic methods in *T. rubrum*.

Homologous recombination (HR), a repair mechanism for DNA double-strand, is one of the most commonly used genetic engineering methods (5). This technique allows the precise insertion of any DNA fragment into the desired genomic region based on sequence homology. Nevertheless, eukaryotes also possess a nonhomologous end-joining (NHEJ) repair mechanism for double-strand breaks, which competes with HR-mediated insertion of DNA into target regions (6). To efficiently promote targeted integration via HR, several fungal species have been engineered by disrupting either of the Ku70/Ku80 complexes involved in NHEJ (7, 8). These strains have demonstrated the effectiveness of improving HR efficiency in various fungi (7, 8).

In this study, we established a highly efficient HR system using a *ku80*-deficient strain of *T. rubrum*. Using this established system, we developed a mutant in which the neomycin phosphotransferase (*nptII*) gene was inserted into the 3□-UTR region of *cyp51A*, which encodes a target for azole antifungals. When the azole antifungal drug efinaconazole was added, the magnitude of increase in *cyp51A* expression decreased in this mutant, which also exhibited

sensitivity to ravuconazole and efinaconazole. This study would accelerate the production of genetically engineered strains to investigate the pathogenicity and drug resistance of *T. rubrum* and provide novel insights into antifungal targets.

MATERIALS AND METHODS

Fungal and bacterial strains and culture conditions

T. rubrum CBS118892 (9), a clinically isolated strain from a patient's nail, was cultured on Sabouraud dextrose agar (SDA; 1% Bacto peptone, 4% glucose, 1.5% agar, pH unadjusted) at 28°C. The conidia of *T. rubrum* were prepared as described previously (10). We confirmed the sequence of *cyp51A* and *cyp51B* as well as their promoters and terminators.

Plasmid construction

To construct a *ku80*-targeting vector, pAg1-Δ*ku80-flp*, approximately 2.1 and 1.5 kb of the 5′- and 3′-UTR fragments, respectively, of the *ku80* open reading frame (ORF) were amplified from *T. rubrum* genomic DNA by polymerase chain reaction (PCR). The PCR products of the 5′- and 3′-UTR fragments were cleaved by *Spe*I/*Apa*I and *Bgl*II/*Kpn*I, respectively. The plasmid backbone of pAg1 and the FLP/FRT module of pMRV-TmKu80/T2 were cleaved by *Spe*I/*Kpn*I and *Apa*I/*Bam*HI, respectively (11). These fragments were joined using Ligation high version 2 (TOYOBO, Japan). To construct a *cyp51A* 3′-UTR-targeting vector, pAg1-*cyp51A*-3′-UTR, the *cyp51A* ORF and 1.5 kb of the 3′-UTR fragment of *cyp51* ORF were amplified from *T. rubrum* genomic DNA by PCR. The *neomycin phosphotransferase* gene cassette, which consists of *E. coli* neomycin phosphotransferase (*nptII*), *Aspergillus nidulans trpC* promoter (*PtrpC*), and *Aspergillus fumigatus cgrA* terminator (*TcgrA*), was cleaved from pMRV-TmKu80/T2 using *Apa*I and *Cla*I. These fragments were joined using an In-Fusion HD Cloning Kit (TaKaRa Bio, Japan). The primers used in this study are shown in Table 1.

Transformation of *T. rubrum*

T. rubrum was transformed using the polyethylene glycol (PEG) method as described previously (12). The desired transformants and purified genomic DNA were analyzed by PCR. Total DNA was extracted using the Quick-DNA Fungal/Bacterial Miniprep Kit (Zymo Research, USA). Fungal cells were disrupted by μT-01 (TAITEC, Japan) using 5-mm stainless beads.

Antifungal susceptibility assay

Conidia (2×10^3) were incubated with two-fold serial dilutions of antifungal agents in 200 μl MOPS-buffered RPMI (pH 7.0) at 28°C for 7 days, and the minimum inhibitory concentration MIC_{100} (concentration required to inhibit growth by 100%) was determined. Efinaconazole was purchased from BLD Pharmatech Ltd, China, and ravuconazole was purchased from Merck.

Quantitative reverse transcription-PCR (qRT-PCR)

Total RNAs were purified using NucleoSpin RNA (Macherey-Nagel) and reverse-transcribed into cDNAs using ReverTra Ace (Toyobo) according to the manufacturers' instructions. qRT-PCR was performed using TB Green Premix Ex Taq II (TaKaRa Bio, Japan) on a StepOne Real-time PCR (Thermo Fisher Scientific, USA). The relative mRNA expression level was determined using the $2^{-\Delta\Delta Ct}$ method using *chitin synthase I* (*csh1*) as an endogenous control to normalize the samples (13). The primers used in this study are listed in Table 1.

Statistical analysis

Mean values of three or more groups with two variables were compared using two-way ANOVA with Šidák correction (for Figure 2A) and Tukey's post hoc test (for Figure 2D), according to the recommendation of Prism 10 (GraphPad, USA). The difference in the efficiency of

126 HR in wild-type (WT) and Δ*ku80* strains was analyzed by two-sided Fisher's exact test using Prism

127 10 (GraphPad, USA). Differences were considered significant at $P < 0.05$.

128

RESULTS

To increase gene targeting efficiency, we attempted to delete the gene encoding Ku80, which promotes nonhomologous recombination repair and whose deletion increases gene targeting efficiency by HR in other fungal species (7, 8). *T. rubrum* CBS 118892 has been isolated from human nail. This strain has been used for whole genome analysis (9) and several transcriptome analyses (14–17), as well as to produce genetically modified strains (18–21). Therefore, we used this strain as a parent strain of *ku80* deletion strain. The *ku80* ORF was replaced with a cassette with the neomycin resistance gene (*nptII*) and *flippase* (*flp*) flanked by flippase recognition sequences (**Fig. 1a**). As *flp* was inserted downstream of the copper ion-responsive promoter P_{ctr4}, *nptII* and *flp* were removed from the *ku80*-deficient genome by adding the copper ion chelator bathocuproinedisulfonic acid to induce FLP recombinase expression (**Fig. 1a**).

To confirm that the *ku80*-deficient strain (*Δku80*) was generated as designed, PCR was performed using genomic DNA purified from WT and *Δku80* strains (**Fig. 1a**, top and bottom, respectively) as templates. PCR performed using WT genomic DNA and primers designed for the 5□- and 3□-UTR of *ku80* (Primers 1 and 2 in **Fig. 1a**, respectively) amplified the PCR products with the expected size (6.6 kbp; **Fig. 1b**, left lane). The size of PCR products in *Δku80* was reduced as expected (3.8 kbp; **Fig. 1b**, right lane). In contrast, PCR performed using primers designed against sequences in the 5□-UTR (Primer 3 in **Fig. 1a**) and the ORF of *ku80* (Primers 4 and 5 in **Fig. 1a**) yielded PCR products of the expected size for WT (**Fig. 1c** and **d**, left lanes) but not for *Δku80* (**Fig. 1c** and **d**, right lanes) strain. The deletion of *nptII* from the genome of *Δku80 + nptII* strain (**Fig. 1a**, middle) was confirmed by PCR using primers designed against the sequences in the promoter and terminator of *nptII* (Primers 6 and 7 in **Fig. 1a**, respectively, **Fig. 1e**). The deletion of *Δku80* was also confirmed by Southern blot analysis of genomic DNA from WT and *Δku80* strains (**Fig. 1f**). These data indicated that the *Δ*ku80 strain was successfully generated with no reduction

in the number of available drug markers. To ascertain the extent of the impact of Ku80 protein on growth, we compared mycelial growth between WT and Δ*ku80* strains, which revealed comparable mycelial growth (**Fig. 1g**).

Azole antifungal drugs used for treating dermatophytosis target the lanosterol demethylase Cyp51, which functions in the ergosterol synthesis pathway. XP_003235929 and XP_003236980 in *T. rubrum* have been identified as Cyp51A and Cyp51B homologs, respectively (22). It has been reported that the addition of azole antifungal drugs induces fungal Cyp51 expression (23, 24). In this study, the mRNA expression of *cyp51A* in *T. rubrum* was upregulated by the addition of the azole antifungal drug efinaconazole, but that of *cyp51B* was not upregulated (**Fig. 2a**). This result suggests that Cyp51A functions as a responsible Cyp51 isozyme when ergosterol biosynthesis is hindered, such as during treatment with azole antifungals. Because the *cyp51* homolog *erg11* is an essential gene in budding yeast, a deficiency of dermatophyte *cyp51A* could cause strong growth defects. In budding yeast, disruption of the natural 3′-UTR by the insertion of an antibiotic-resistant marker was found to destabilize the corresponding mRNAs, and this strategy has been used to analyze essential genes (25, 26). We attempted to insert the *neomycin phosphotransferase* (*nptII*) gene cassette into the downstream of *cyp51A* ORF of *T. rubrum*, as demonstrated in budding yeast studies (25, 26). Using the obtained Δ*ku80* strain, we inserted a *nptII* cassette into *cyp51A* 3′-UTR (hereinafter termed the 3′-UTR disruptant; **Fig. 2b** and **c**). Homologous recombinant strains were obtained in 12 of 26 strains (46.2%; Table 2) in which the insertion of the drug resistance gene was confirmed by PCR using primers designed within the ORF and 3′-UTR of *cyp51A* (Primers 8 and 9, respectively; **Fig. 2b** and **c**). The HR efficiency of the Δ*ku80* strain was 46 times higher than that of the WT strain (1/98; 1.0%; Table 2). These data demonstrated that a highly efficient HR method had been established in *T. rubrum*.

176 The mRNA level of *cyp51A* in the 3′-UTR disruptant was comparable to that in the parent
177 strain Δ*ku80* (**Fig. 2d**). Nevertheless, efinaconazole-induced elevation of *cyp51A* mRNA level
178 decreased in the 3′-UTR disruptant (**Fig. 2d**). These findings suggest that the lack of the 3′-UTR
179 causes mRNA perturbation at least under the condition of *cyp51A* induction in *T. rubrum*. Previous
180 research has reported increased sensitivity to the azole antifungals fluconazole and itraconazole by
181 the suppression of *cyp51A* expression in *A. fumigatus*, which has two Cyp51 isozymes, Cyp51A
182 and Cyp51B, similar to that in *T. rubrum* (27). The 3□-UTR disruptant exhibited similar mycelial
183 growth as that of the *Δku80* strain (**Fig. 2e**), but it showed increased sensitivity to the azole
184 antifungals efinaconazole and ravuconazole (Table 3). However, the MICs of itraconazole and
185 luliconazole remained unchanged. These findings suggest that Cyp51A functions as a factor for
186 azole antifungal tolerance in *T. rubrum*.
187

DISCUSSION

T. rubrum is an anthropophilic dermatophyte specialized for human parasitism, whereas several other dermatophytes are zoophilic or geophilic (28). The nature of this fungus is of great interest from not only a medical but also biological point of view. In recent years, transcriptomic, proteomic, and immunological studies of this fungus have been conducted extensively (17, 29–34). Nevertheless, molecular and cellular biological studies of *T. rubrum* have been limited partially due to a lack of genetic tools for this organism. In this study, we generated a *ku80*-deficient strain of this fungus and demonstrated that this strain can be applied in efficient HR methods, similar to a system established in a zoophilic dermatophyte, *T. mentagrophytes* (formerly *Arthroderma vanbreuseghemii*) (35). The method established in this study might serve as a fundamental technique to promote research that will advance the findings of previous comprehensive analyses and immunological analyses observed on the host side (17, 29–34).

The 3′-UTR disruptant, in which the expression induction of *cyp51A* by efinaconazole was attenuated, exhibited increased sensitivity to efinaconazole and ravuconazole. Considering that *cyp51A* expression was upregulated in response to efinaconazole addition, we speculated that *T. rubrum* Cyp51A is an inducible Cyp51 isozyme crucial for tolerance to azole antifungals. In *A. fumigatus*, loss or suppression of *cyp51A* expression enhances sensitivity to the azole antifungal fluconazole (27). Conversely, *cyp51B* deficiency does not significantly alter fluconazole sensitivity (27). This difference may be partially explained by the lower binding affinity of Cyp51A for fluconazole than for Cyp51B (36). Nevertheless, a difference in the induction of the expression of each *cyp51* gene in response to azoles may also contribute to this disparity in sensitivity. Regarding *T. rubrum*, no studies have investigated the contribution of Cyp51A and Cyp51B isozymes to the resistance to azole antifungal drugs. In the future, it is important to generate *T. rubrum* strains that

211 are deficient in *cyp51A* and *cyp51B*, followed by analyzing their involvement in growth and

212 resistance to azole antifungal drugs.

213

214

215

• Acknowledgments

The authors thank H. Uga, N. Hori, H. Hamanaka for their technical help. This work was supported by the Japan Society for the Promotion of Science.

• Author Contribution Statement

MI conceived and designed research. MI conducted experiments. MI, TY and SO analyzed data. MI, TY and SO wrote the manuscript. All authors read and approved the manuscript.

• Conflicts of Interest (COI)

The authors declare no conflicts of interest.

References

1. Havlickova B, Czaika VA, Friedrich M. 2008. Epidemiological trends in skin mycoses worldwide. Mycoses 51:2–15.
2. Zhan P, Liu W. 2017. The Changing Face of Dermatophytic Infections Worldwide. Mycopathologia2016/10/25. 182:77–86.
3. Monod M, Feuermann M, Salamin K, Fratti M, Makino M, Alshahni MM, Makimura K, Yamada T. 2019. *Trichophyton rubrum* Azole Resistance Mediated by a New ABC Transporter, TruMDR3. Antimicrob Agents Chemother 63:e00863-19.
4. Yamada T, Maeda M, Alshahni MM, Tanaka R, Yaguchi T, Bontems O, Salamin K, Fratti M, Monod M. 2017. Terbinafine Resistance of *Trichophyton* Clinical Isolates Caused by Specific Point Mutations in the Squalene Epoxidase Gene. Antimicrob Agents Chemother 61:e00115-17.
5. Smithies O, Gregg RG, Boggs SS, Koralewski MA, Kucherlapati RS. 1985. Insertion of DNA sequences into the human chromosomal β-globin locus by homologous recombination. Nature 317:230–234.
6. Krappmann S. 2007. Gene targeting in filamentous fungi: the benefits of impaired repair. Fungal Biol Rev 21:25–29.
7. Matsumoto Y, Nagamachi T, Yoshikawa A, Yamazaki H, Yamasaki Y, Yamada T, Sugita T. 2021. Development of an efficient gene-targeting system for elucidating infection mechanisms of the fungal pathogen *Trichosporon asahii*. Sci Rep 11:18270.
8. Yamada T, Makimura K, Satoh K, Umeda Y, Ishihara Y, Abe S. 2009. *Agrobacterium* tumefaciens-mediated transformation of the dermatophyte, Trichophyton mentagrophytes: an efficient tool for gene transfer. Med Mycol 47:485–494.
9. Martinez DA, Oliver BG, Gräser Y, Goldberg JM, Li W, Martinez-Rossi NM, Monod M, Shelest E, Barton RC, Birch E, Brakhage AA, Chen Z, Gurr SJ, Heiman D, Heitman J, Kosti I, Rossi A, Saif S, Samalova M, Saunders CW, Shea T,

Summerbell RC, Xu J, Young S, Zeng Q, Birren BW, Cuomo CA, White TC. 2012. Comparative genome analysis of *Trichophyton rubrum* and related dermatophytes reveals candidate genes involved in infection. mBio2012/09/04. 3:e00259-12.

10. Uchida K, Tanaka T, Yamaguchi H. 2003. Achievement of complete mycological cure by topical antifungal agent NND-502 in guinea pig model of tinea pedis. Microbiol Immunol 47:143–146.
11. Yamada Y, Maeda M, Alshahni MM, Monod M, Staib P, Yamada T. 2014. Flippase (FLP) recombinase-mediated marker recycling in the dermatophyte *Arthroderma vanbreuseghemii*. Microbiology (N Y) 160:2122–2135.
12. Yamada T, Makimura K, Hisajima T, Ito M, Umeda Y, Abe S. 2008. Genetic transformation of the dermatophyte, *Trichophyton mentagrophytes*, based on the use of G418 resistance as a dominant selectable marker. J Dermatol Sci2007/12/04. 49:53–61.
13. Jacob TR, Peres NTA, Persinoti GF, Silva LG, Mazucato M, Rossi A, Martinez-Rossi NM. 2012. rpb2 is a reliable reference gene for quantitative gene expression analysis in the dermatophyte *Trichophyton rubrum*. Med Mycol 50:368–377.
14. Persinoti GF, de Aguiar Peres NT, Jacob TR, Rossi A, Vêncio RZ, Martinez-Rossi NM. 2014. RNA-sequencing analysis of *Trichophyton rubrum* transcriptome in response to sublethal doses of acriflavine. BMC Genomics 15:S1.
15. Mendes NS, Bitencourt TA, Sanches PR, Silva-Rocha R, Martinez-Rossi NM, Rossi A. 2018. Transcriptome-wide survey of gene expression changes and alternative splicing in *Trichophyton rubrum* in response to undecanoic acid. Sci Rep 8:2520.
16. Martins MP, Silva LG, Rossi A, Sanches PR, Souza LDR, Martinez-Rossi NM. 2019. Global Analysis of Cell Wall Genes Revealed Putative Virulence Factors in the Dermatophyte *Trichophyton rubrum*. Front Microbiol 10:2168.
17. Cao X, Xu X, Dong J, Xue Y, Sun L, Zhu Y, Liu T, Jin Q. 2022. Genome-wide identification and functional analysis of circRNAs in *Trichophyton rubrum* conidial and mycelial stages. BMC Genomics 23:21.

18. Lang EAS, Bitencourt TA, Peres NTA, Lopes L, Silva LG, Cazzaniga RA, Rossi A, Martinez-Rossi NM. 2020. The stuA gene controls development, adaptation, stress tolerance, and virulence of the dermatophyte *Trichophyton rubrum*. Microbiol Res 241:126592.
19. Ishii M, Matsumoto Y, Yamada T, Uga H, Katada T, Ohata S. 2023. TrCla4 promotes actin polymerization at the hyphal tip and mycelial growth in *Trichophyton rubrum*. Microbiol Spectr e02923-23.
20. Ishii M, Yamada T, Ishikawa K, Ichinose K, Monod M, Ohata S. 2024. The Ptk2-Pma1 pathway enhances tolerance to terbinafine in *Trichophyton rubrum*. Antimicrob Agents Chemother 0:e01609-23.
21. Ishii M, Matsumoto Y, Yamada T, Uga H, Katada T, Ohata S. 2024. Targeting dermatophyte Cdc42 and Rac GTPase signaling to hinder hyphal elongation and virulence. bioRxiv https://doi.org/10.1101/2024.03.04.583433.
22. Celia-Sanchez BN, Mangum B, Brewer M, Momany M. 2022. Analysis of Cyp51 protein sequences shows 4 major Cyp51 gene family groups across fungi. G3 Genes|Genomes|Genetics 12:jkac249.
23. Roundtree TM, Juvvadi RP, Shwab KE, Cole CD, Steinbach JW. 2020. Aspergillus fumigatus Cyp51A and Cyp51B Proteins Are Compensatory in Function and Localize Differentially in Response to Antifungals and Cell Wall Inhibitors. Antimicrob Agents Chemother 64:10.1128/aac.00735-20.
24. Henry WK, Nickels TJ, Edlind DT. 2000. Upregulation of ERG Genes inCandida Species by Azoles and Other Sterol Biosynthesis Inhibitors. Antimicrob Agents Chemother 44:2693–2700.
25. Schuldiner M, Collins SR, Thompson NJ, Denic V, Bhamidipati A, Punna T, Ihmels J, Andrews B, Boone C, Greenblatt JF, Weissman JS, Krogan NJ. 2005. Exploration of the Function and Organization of the Yeast Early Secretory Pathway through an Epistatic Miniarray Profile. Cell 123:507–519.
26. Breslow DK, Cameron DM, Collins SR, Schuldiner M, Stewart-Ornstein J, Newman HW, Braun S, Madhani HD, Krogan NJ, Weissman JS. 2008. A comprehensive

strategy enabling high-resolution functional analysis of the yeast genome. Nat Methods 5:711–718.

27. Hu W, Sillaots S, Lemieux S, Davison J, Kauffman S, Breton A, Linteau A, Xin C, Bowman J, Becker J, Jiang B, Roemer T. 2007. Essential Gene Identification and Drug Target Prioritization in *Aspergillus fumigatus*. PLoS Pathog 3:e24-.
28. Errol Reiss, H. Jean Shadomy GML. 2011. Dermatophytosis, p. 527–565. *In* Fundamental Medical Mycology. Wiley-Blackwell.
29. Burstein VL, Beccacece I, Guasconi L, Mena CJ, Cervi L, Chiapello LS. 2020. Skin Immunity to Dermatophytes: From Experimental Infection Models to Human Disease. Front Immunol 11:605644.
30. Martinez-Rossi NM, Peres NTA, Bitencourt TA, Martins MP, Rossi A. 2021. State-of-the-Art Dermatophyte Infections: Epidemiology Aspects, Pathophysiology, and Resistance Mechanisms. J Fungi (Basel) 7.
31. Galvão-Rocha FM, Rocha CHL, Martins MP, Sanches PR, Bitencourt TA, Sachs MS, Martinez-Rossi NM, Rossi A. 2023. The Antidepressant Sertraline Affects Cell Signaling and Metabolism in Trichophyton rubrum. Journal of Fungi 9.
32. Peres NTA, Lang EAS, Bitencourt TA, Oliveira VM, Fachin AL, Rossi A, Martinez-Rossi NM. 2022. The bZIP Ap1 transcription factor is a negative regulator of virulence attributes of the anthropophilic dermatophyte *Trichophyton rubrum*. Curr Res Microb Sci 3:100132.
33. Xu X, Hu X, Dong J, Xue Y, Liu T, Jin Q. 2022. Proteome-Wide Identification and Functional Analysis of Lysine Crotonylation in *Trichophyton rubrum* Conidial and Mycelial Stages. Front Genet 13.
34. Xu X, Liu T, Yang J, Chen L, Liu B, Wang L, Jin Q. 2018. The First Whole-Cell Proteome- and Lysine-Acetylome-Based Comparison between *Trichophyton rubrum* Conidial and Mycelial Stages. J Proteome Res 17:1436–1451.
35. Yamada T, Makimura K, Hisajima T, Ishihara Y, Umeda Y, Abe S. 2009. Enhanced gene replacements in Ku80 disruption mutants of the dermatophyte, *Trichophyton mentagrophytes*. FEMS Microbiol Lett 298:208–217.

36. Andrew SWG, Melo N, Martel MC, Parker EJ, Nes DW, Kelly LS, Kelly ED. 2010. Expression, Purification, and Characterization of *Aspergillus fumigatus* Sterol 14-α Demethylase (CYP51) Isoenzymes A and B. Antimicrob Agents Chemother 54:4225–4234.

Figure 1 *ku80* locus targeting and *nptII* marker excision.

(A) Schematic representation of the *ku80* locus before and after excision of flipper modules in *T. rubrum*. Site-specific recombination between the flanking FRT sequences (black box) was performed by the conditional expression of *flp*.

(B–E) PCR analysis of total DNA samples from transformants. WT was used as a control. (B) Fragments were amplified with primer pairs (Primers 1 and 2). (C) Fragments were amplified with primer pairs (Primers 3 and 4). (D) Internal fragments of the *ku80* ORF were amplified with primer pairs (Primers 5 and 4). (E) Internal fragments of *nptII* were amplified with primer pairs (Primers 6 and 7). The *nptII*-harboring strain (Δ*cla4*) was used as a positive control.

(F) Southern blot analysis of genome DNA samples from wild-type and Δ*ku80* strains.

(G) Mycelial growth of WT and Δ*ku80* strains on SDA at 28°C for 16 days.

Figure 2 Production and characterization of the *cyp51A* 3□-UTR disruptant of *T. rubrum*.

(A) The mRNA expression of *cyp51A* and *cyp51B* with or without 1/10 MIC of efinaconazole in WT. Data are expressed as mean ± SD. The dots on the graph represent biological replicates (n = 4). n.s., not significant. ****, P < 0.0001.

(B) Schematic representation of the *cyp51A* locus of WT and *cyp51A* 3□-UTR disruptant (3□-UTR disruptant).

(C) PCR analysis of total DNA samples from the 3□-UTR disruptant. The fragments were amplified with primer pairs (Primer 8 and 9). Δ*ku80* was used as a control.

(D) The mRNA expression of *cyp51A* in Δ*ku80* and *cyp51A* 3□-UTR disruptant (3□-UTR) with or without 1/10 MIC of efinaconazole. The bars represent the standard deviation of the data obtained from three independent experiments. Data are expressed as mean ± SD. The dots on the graph represent biological replicates (n = 4–10). n.s., not significant. ****, P□<□0.0001.

(E) Mycelial growth of Δ*ku80* and *cyp51A* 3□-UTR disruptant on SDA at 28□ for 13 days.

Table 1 Primers used in this study.

Primer name	Sequences
ku80-5□-F-*Spe*I	5□-CGC ACT AGT CCA CTG GAG ATC CCC AAC AG-3□
ku80-5□-R-*Apa*I	5□-CGC GGG CCC TCG GGT CAA ACA GCC ACA AT-3□
ku80-3□-F-*Bgl*II	5□-CGC AGA TCT GCT GCT GGT GGG TAT GTA GG-3□
ku80-3□-R-*Kpn*I	5□-CGC GGT ACC TTC GTT TGA GCC GAG AGA CC-3□
cyp51A-F-*Spe*I	5□-ACT AGT ATG GCC GTG CTC ACA GTG-3□
cyp51A-R-*Apa*I	5□-GGG CCC TAA CGT GAA TTA GAA CGT CGT TC-3□
cyp51A-3□-F-*Cla*I	5□-CGA TCG ATA CTC ACA GTT ATT GAA CAG TTT CTG TA-3□
cyp51A-3□-R-*Kpn*I	5□-GCG GGT ACC AGC TCG GAA ATG CCT TGA CA-3□
Primer 1	5□-TGA GGA AGG CCA GGG GAA CTT AT-3□
Primer 2	5□-CCT TCC TGC TCT TTG CTT TCC CT-3□
Primer 3	5□-AGC TGG TCT CGG AAA GTT GG-3□
Primer 4	5□-AAG CCA CCA AAG CTC TCT CC-3□
Primer 5	5□-AGC TCC TTC AAT TGA CCC GG-3□
Primer 6	5□-AGA TGA TTC ATG ACG TAT ATT CAC CG-3□
Primer 7	5□-GAT GGA TTG CAC GCA GGT TC-3□
Primer 8	5□-CAC TGT TTT CTG GAC CTA TGA AAC C-3□
Primer 9	5□-GCG AAT ACA GCA GAG AGA AAA TTG A-3□
chs1-RT-F	5□-GGC CAC AAC GAA GCC TAT GA-3□
chs1-RT-R	5□-GCT GGG AGG TAC TGT TTG ATC AA-3□
cyp51A-RT-F	5□-CAA TCG GCC TGG GAG ATG-3□
cyp51A-RT-R	5□-TTG GAC TTA GCT CCT TCG CG-3□
cyp51B-RT-F	5□-GAA CAA CGT TGG TGT CAC CG-3□
cyp51B-RT-R	5□-ACA TCT GTG TCT GCC TGA GC-3□

Table 2 Gene targeting efficiency of WT and Δ*ku80* strains.

Strain	Total transformants	Homologous replacement	Efficiency (%)
WT	98	1	1.0
Δ*ku80*	26	12	46.2

*Two-sided Fisher's exact test, $P < 0.0001$

Table 3 MIC values (μg/ml) of efinaconazole and ravuconazole in Δ*ku80* and *cyp51A* 3□-UTR disruptants (3□-UTR disruptants).

Azole drugs	Δ*ku80*	3□-UTR disruptant #1
Efinaconazole	0.010	0.0025
Ravuconazole	0.040	0.020
Itraconazole	0.50	0.50
Luliconazole	0.00063	0.00063

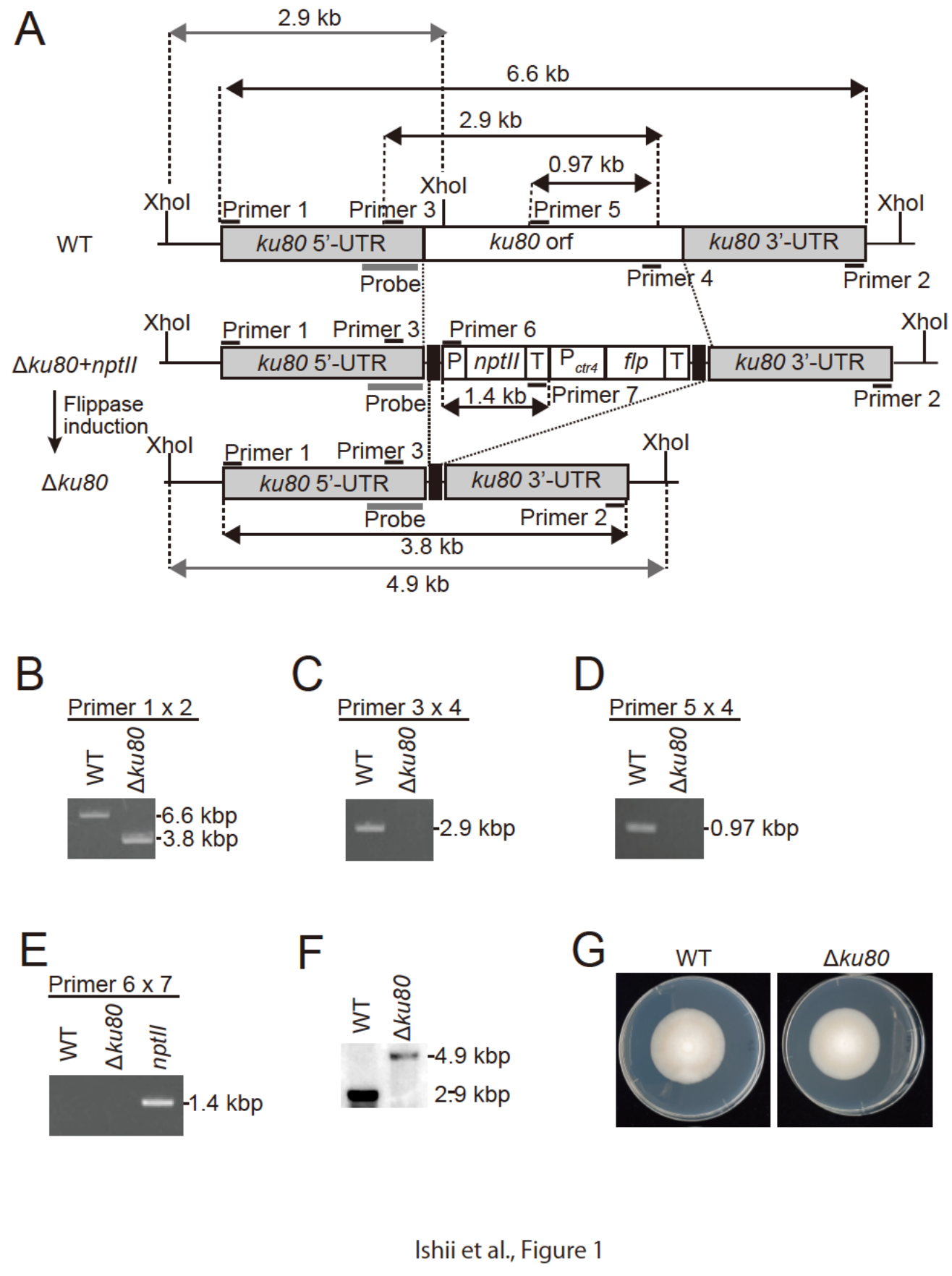

Ishii et al., Figure 1

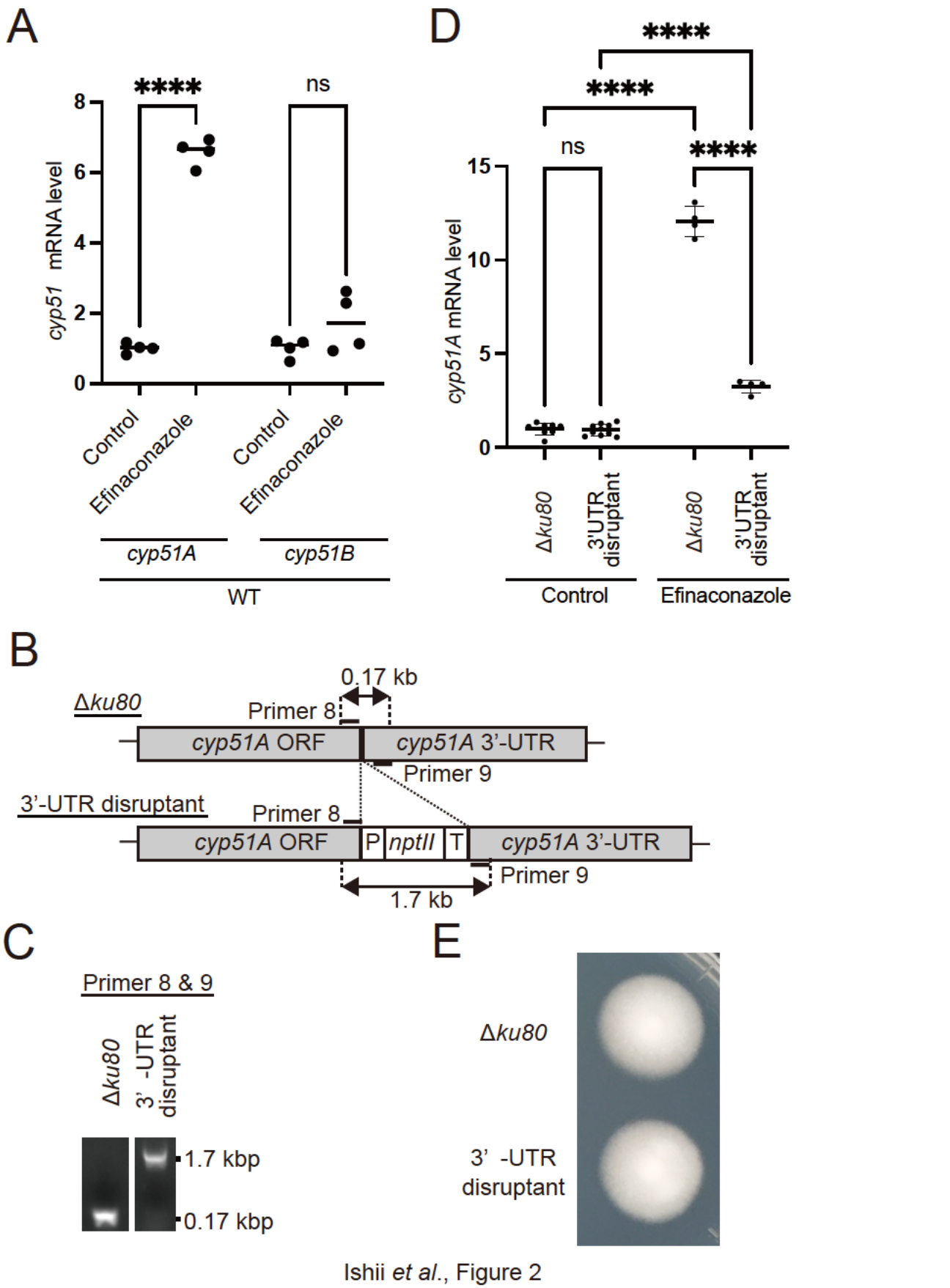

Ishii *et al.*, Figure 2